energies

MDPI

Article

Analysis of Convergence Characteristics of Average Method Regulated by ISO 9869-1 for Evaluating In Situ Thermal Resistance and Thermal Transmittance of Opaque Exterior Walls

Doo Sung Choi [1] and Myeong Jin Ko [2,*]

1 Department of Architectural Engineering, Chungwoon University, Incheon 22100, Korea; trebelle@chungwoon.ac.kr
2 Department of Building System Technology, Daelim University College, Anyang 13916, Korea
* Correspondence: whistlemj@nate.com; Tel.: +82-31-467-4825

Received: 17 March 2019; Accepted: 21 May 2019; Published: 24 May 2019

check for updates

Abstract: In the last few decades, an average method which is regulated by ISO 9869-1 has been used to evaluate the in situ thermal transmittance (*U*-value) and thermal resistance (*R*-value) of building envelopes obtained from onsite measurements and to verify the validity of newly proposed methods. Nevertheless, only a few studies have investigated the test duration required to obtain reliable results using this method and the convergence characteristics of the results. This study aims to evaluate the convergence characteristics of the in situ values analyzed using the average method. The criteria for determining convergence (i.e., end of the test) using the average method are very strict, mainly because of the third condition, which compares the deviation of two values derived from the first and last periods of the same duration. To shorten the test duration, environmental variables should be kept constant throughout the test or an appropriate period should be selected. The convergence of the in situ *U*-value and *R*-value is affected more by the length of the test duration than by the temperature difference if the test environment meets literature-recommended conditions. Furthermore, there is no difference between the use of the *U*-value and *R*-value in determining the end of the test.

Keywords: thermal resistance; thermal transmittance; heat flow meter method; average method; convergence characteristics; opaque exterior wall

1. Introduction

To promote the spread of energy-efficient buildings, many countries around the world have enacted regulations and established policies. One of the most prominent and easy approaches by most countries is the imposition of increasingly strict specifications on the thermal performance of buildings. That is, the minimum required performance level of a building envelope has been tightened considerably over the past decade. For example, the mandatory thermal transmittance (*U*-value) for the exterior walls of residential buildings in Seoul, South Korea, has reduced from 0.48 W/m^2·K in 2008 to 0.17 W/m^2·K in 2018 [1].

The *U*-value is one of the most important properties used to evaluate the thermal performance of a building envelope. This property can be determined by theoretical or experimental methods. The theoretical *U*-value can be estimated using an approach regulated by the ISO 6946 standard [2] based on an electrical analogy and a steady-state condition. The theoretical *U*-value is used in the approval process for newly constructed or refurbished structures and in the certification process for energy-efficient buildings. However, these theoretical values do not accurately represent the in situ *U*-values because of various reasons associated with the design, construction, and operational stages.

The discrepancies between the theoretical and in situ values provide misleading information on the energy performance of buildings, which not only prevents the owner from establishing a reasonable energy consumption plan but also may lead to economic losses resulting from missing the renovation period and selecting inappropriate retrofitting activities [3]. In particular, condensation has occurred even in recently constructed buildings with low theoretical *U*-values which have been certified as energy-efficient buildings; this indicates the limitations of the theoretical method and the importance of onsite measurement of *U*-values.

The heat flow meter method, which is regulated by the ISO 9869-1 standard [4], is a widely used method to measure the in situ *U*-value of building envelopes. This method estimates the in situ *U*-value by analyzing the measurement data of the heat flux through a test wall and the temperature difference between the inside and outside environments. According to the ISO standard, if the environmental condition is stable, the test should last at least 3 days; otherwise, the minimum test duration may be more than 7 days to obtain reliable results.

Many studies have previously evaluated the in situ *U*-value of walls using the standardized average method and compared the value with the theoretical value. For example, in a study by Adhikari et al. [5] on historical building walls, the differences between theoretical and measured *U*-values ranged from 2% to 58%. Cabeza et al. [6] measured the in situ *U*-values of experimental cubicles that used three typical insulation materials, namely polyurethane, polystyrene, and mineral wool. They found that the average differences between the experimental and theoretical *U*-values in two different weeks were 12% and 14%. Asdrubali et al. [7] conducted a study on some green buildings with low calculated *U*-values and found that the differences between the calculated and measured *U*-values ranged from 4% to 75%. Evangelisti et al. [8] evaluated the in situ *U*-values of three conventional exterior walls in the range of 0.504–1.897 W/m^2·K. They reported that the discrepancies between the theoretical *U*-value and measured *U*-value were in the range of 17–153%. Baker [9] evaluated the in situ *U*-values of traditional Scottish stone masonries with theoretical *U*-values ranging from 0.30 W/m^2·K to 2.65 W/m^2·K. The results showed that 44% of the total number of measurements were lower than the calculated *U*-value range, 42% were within the calculated range, and 14% were higher than the calculated range. Rye and Scott [10] reported that in 77% of the measurement cases, the software overestimated the *U*-values compared to onsite measurements. Other studies [11–14] have reported similar results that show discrepancies between theoretical and measured *U*-values, although the degree of discrepancy differs.

The above literature review indicates that many researchers have used the average method defined by the ISO 9869-1 standard [4] for data-processing. However, because the average method does not take into account the dynamic behavior of the walls, the test duration usually needs to be extended to improve the estimation accuracy of the in situ *U*-value. Therefore, the proper test duration and factors influencing the value are very interesting research topics. A study conducted by Rye and Scott [10] on traditional Scottish masonries showed that a period of at least a week is required before the *U*-value estimate stabilizes to within ±5% of the final value determined from data gathered over approximately 27 days. Asdrubali et al. [7] reported that when using the average method, the acquisition time can be 3 days if the indoor temperature is stable; otherwise, the time interval must be extended to 7 days. Gaspar et al. [12] showed that in the measurements of low *U*-value façades, temperature differences of above 19 °C require a test duration of 72 h; however, for lower temperature differences, the test duration must be extended to 144 h. Ahmad et al. [13] evaluated the in situ *U*-value and thermal resistance (*R*-value) of north- and east-facing walls made from reinforced precast concrete panels using the average method. The results showed that a test period of 6 days is sufficient to ascertain the in situ *U*-value and *R*-value of reinforced precast concrete walls. The results also indicated that, where the *U*-value depends on the wall orientation and outside weather conditions, the *R*-value is independent of the wall orientation. Ficco et al. [14] conducted in situ *U*-value measurements on existing buildings with theoretical *U*-values ranging from 0.37 W/m^2·K to 3.30 W/m^2·K. They estimated high relative uncertainties ranging from 8% at optimal operating conditions to approximately 50%

at nonoptimal operating conditions. They also reported that temperature differences lower than 10 °C and low heat flow lead to unacceptable uncertainties. Deconinck and Roels [15] compared the performance of several semi-stationary and dynamic data analysis techniques used for evaluating the thermal property of building components using simulated datasets with different lengths and for different seasons. An analysis of the *R*-value using the average method showed that data periods of around 20 days or longer are required to obtain 5% accurate results in January. The simulation results also indicated that the *R*-values for the two summer scenarios in July showed the limited validity of the average method. Gaspar et al. [16] evaluated the minimum duration of in situ experimental campaigns to measure the *U*-value of the façades of existing buildings using the heat flow meter method. They determined the minimum test duration according to the criteria of data quality and variability of results proposed in ASTM C1155 [17] and the three convergence conditions described in ISO 9869-1 [4]. The results showed that the ISO criteria are more sensitive and provide more accurate results than the ASTM criteria but require a longer test duration.

The infrared thermography (IRT) method is widely employed in building diagnostics for qualitative evaluation to detect heat losses, air leakages, thermal bridges, sources of moisture, missing materials, and defects in insulation materials [18–22]. Furthermore, many studies [23–28] have recently proposed quantitative IRT methodologies for evaluating the in situ *U*-value of a building envelope. In addition, several researchers [29–31] have proposed the use of statistical approaches, in particular Bayesian inference, to infer the in situ thermal properties from heat flux and temperature measurements. It is noteworthy that the validity of these newly proposed methods is mainly verified using the average method, which is regulated by ISO 9869-1 [4].

The above literature review shows that many researchers have used the average method to obtain the in situ *U*-values and have reported the minimum measurement period and environmental conditions required when this method is used. The average method has also been used for the verification of newly proposed methods. Nevertheless, with regard to determining the in situ *U*-values using the average method, studies on the test duration required to obtain a reliable result and the causes that increase the test duration are still lacking. Furthermore, only a few works have investigated the convergence characteristics of the in situ *U*-value or *R*-value.

Therefore, this study aims to evaluate the convergence characteristics of the in situ *R*-value and *U*-value of an exterior wall analyzed using the average method as a data-processing technique. The convergence characteristics were analyzed according to the convergence conditions of the ISO 9869-1 standard [4] using datasets with different analysis periods in a measurement campaign of 21 consecutive days. In addition, the convergence characteristics of both the *R*-value and *U*-value were reviewed together to identify the difference between the use of the two values for determining the end of the test. A clearer understanding of the convergence characteristics will help researchers and diagnosticians to select an appropriate test duration and reduce the uncertainty of onsite measurements of the *R*-value and *U*-value.

The rest of this paper is organized as follows. Section 2 describes the case study and the method used in the research. Section 3 discusses the convergence characteristics of both the *R*-value and *U*-value. Finally, Section 4 presents the conclusions of the study and future research ideas.

2. Methods

2.1. Investigated Building

The building considered in this case study was a private house with a 52 m^2 floor area, which was constructed in 1990 and is located in the city of Gwangmyeong in the central region of Korea. The test object was the northwest-facing external wall to avoid direct solar radiation. Table 1 lists the materials of the test wall and their thermal conductivity, as well as their *R*-value and *U*-value calculated using the theoretical approach regulated by ISO 6946 [2]. Information on the building materials and surface resistances was obtained from the design documents. The calculated *U*-value can be determined as follows:

$$U_D = \frac{1}{R_{si} + \sum_i \frac{t_i}{\lambda_i} + R_{se}}, \tag{1}$$

where U_D represents the U-value evaluated by the calculation method (W/m^2·K); t_i is the thickness of the i-th layer (m); λ_i is its thermal conductivity (W/m·K); and R_{si} and R_{se} are the interior and exterior surface resistances (m^2·K/W), respectively.

Table 1. Stratigraphies and thermophysical properties of the test wall.

Material Layer	t	λ	ρ	c	R	U_D (W/m^2·K)
Internal surface					0.110	
Mortar	10	1.400	2000	780	0.007	
Cement brick	90	0.600	1700	835	0.150	0.460
Glass wool	60	0.035	40	670	1.714	
Cement brick	90	0.600	1700	835	0.150	
External surface					0.043	

t: Thickness; λ: Thermal conductivity; ρ: Density; c: Specific heat capacity; R: Thermal resistance; U_D: Theoretical thermal transmittance.

2.2. In Situ Measurement

Onsite measurement was conducted from December 30, 2016 to January 19, 2017 in accordance with the ISO 9869-1 standard [4]. The standard states that surveys can last from a minimum of 3 days to more than 7 days. However, many studies [7,8,12–14,28,29] conducted measurements for approximately 1 week and sometimes even more than 2 weeks to obtain satisfactory results. In this study, the measurement was conducted for 21 days to identify the effects of increases and changes in the measurement period.

The measurement equipment consisted of devices for measuring the R-value and U-value, such as a heat flux sensor and temperature sensor, and devices for confirming the validity of the measurement conditions, such as a pyranometer and an infrared camera. The heat flux sensor (EKO MF-200, EKO Instruments, Tokyo, Japan) was installed on the inside surface of the test wall after identifying the best position using the infrared camera (FLIR T620, FLIR systems, Portland, OR, USA). Two thermocouples (Testo 0602 5792, Testo AG, Lenzkirch, Germany) were mounted on the inside surface near the heat flux sensor and on the opposite outside surface with adhesive tape. The inside air temperature and wind speed were measured in the vicinity of the test wall using a comfort probe (Testo 0628 0143, Testo AG, Lenzkirch, Germany). A hot-wire anemometer (Testo 0635 1543, Testo AG, Lenzkirch, Germany) was employed to measure the outside air temperature and local wind speed. The pyranometer (EKO MS 602, EKO Instruments, Tokyo, Japan) was installed perpendicular to the outside surface to identify the influence of direct solar radiation. The measurements were recorded using a data logger (Graphtec GL220, Graphtec Corporation, Yokohama, Japan) with a sampling period of 1 min. The main technical specifications of the measurement equipment are listed in Table 2, whereas Figure 1 shows the installation of the measurement equipment.

Table 2. Main technical specifications of measurement equipment.

Equipment (model)	Parameter	Range	Accuracy
Heat flux sensor (EKO MF-200)	Heat flux		±2%
Comfort probe (Testo 0628-0143)	Inside air temperature Inside wind speed	0–50 °C 0–5 m/s	±0.5 °C ± (0.03 m/s + 4%)
Hot-wire probe (Testo 0635-1543)	Outside air temperature Outside wind speed	−20–70 °C 0–20 m/s	±0.5 °C ±(0.03 m/s + 4%)
Thermocouple (Testo 0602-5792)	Surface temperature	−200–1000 °C	±(0.5 °C + 0.3%)
Pyranometer (EKO MS-602)	Solar radiation	0–2000 W/m^2	<25 W/m^2
Infrared camera (FLIR T-620)	Thermogram	7.5–14 µm	±2 °C

Figure 1. Photograph of the test wall and measurement equipment.

The measured data obtained from the 21 days of the experimental campaign are shown in Figure 2. The average air and surface temperature differences between the inside and outside environments throughout the monitoring period were 21.8 °C and 19.6 °C, respectively. These temperature differences were considerably higher than the recommended value of 10 °C. The maximum solar radiation incident on the outside surface of the northwest-facing test wall was 109.8 W/m^2; thus, the influence of direct solar radiation was considered negligible. The average indoor and outdoor wind speeds were approximately 0.07 m/s and 0.23 m/s, respectively. In particular, the average outdoor wind speed was significantly lower than the recommended value of 1 m/s to avoid excessive effects of convective phenomena. In addition, the influence of moisture content on the measurement results is considered negligible, as there was no rain during the measurement period.

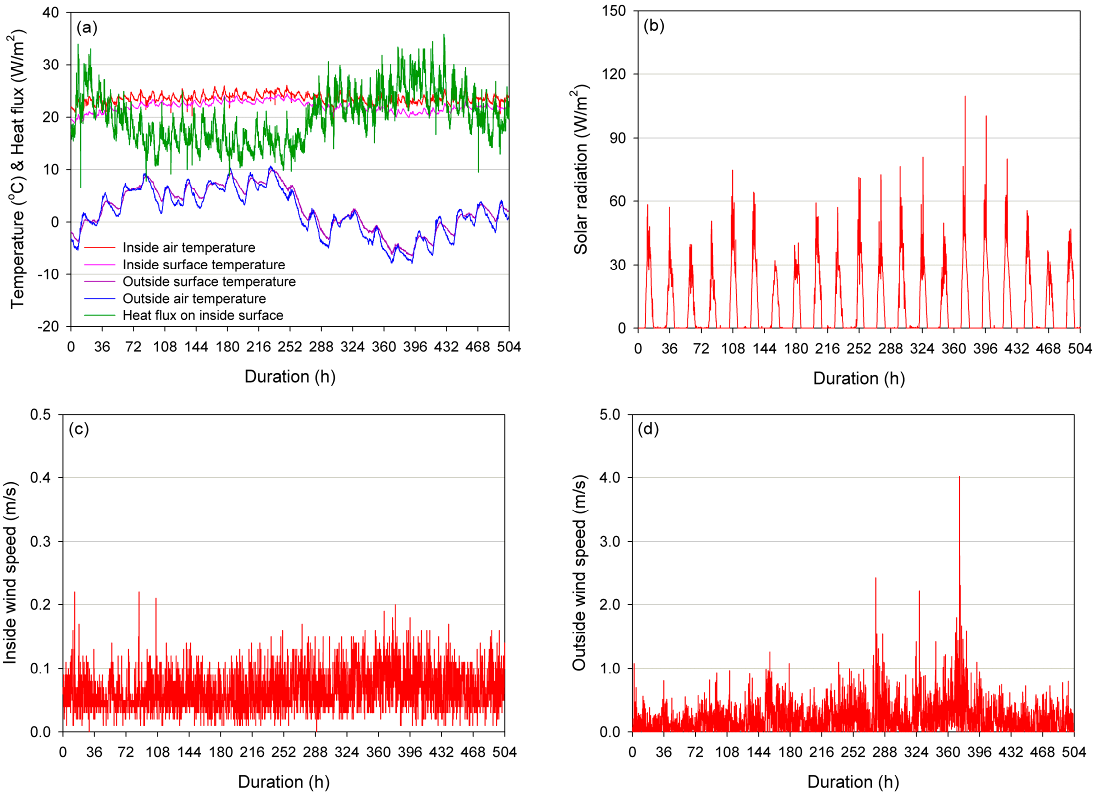

Figure 2. Data obtained from the monitoring process from December 30, 2016 to January 19, 2017: (**a**) Temperature and heat flux; (**b**) solar radiation; (**c**) inside wind speed; and (**d**) outside wind speed.

2.3. Data Analysis

The U-value was analyzed using the average method regulated by ISO 9869-1 [4]. The average method assumes that the U-value can be obtained by dividing the mean density of the heat flow rate by the mean temperature difference. If the average is taken over a sufficiently long period of time, a good estimation of the equivalent steady-state thermal behavior of the wall can be obtained. An estimate of the in situ U-value can be obtained as follows:

$$U_{AM} = \frac{\sum_{j=1}^{n} q_j}{\sum_{j=1}^{n} \left(T_{i,j} - T_{e,j}\right)}, \tag{2}$$

where U_{AM} represents the U-value evaluated by the average method (W/m^2·K); q is the density of the heat flow rate (W/m^2); T_i and T_e are the interior and exterior air temperatures (K), respectively; and j represents the individual measurements.

According to the ISO 9869-1 standard [4], the end of the test should be determined using the R-value calculated from the surface temperature difference across the test wall. However, even though the difference between the use of the two values in determining when to terminate the test is not clearly known, several researchers [7,8,12,16] used the U-value instead of the R-value. An estimate of the R-value is obtained as follows:

$$R_{AM} = \frac{\sum_{j=1}^{n} \left(T_{si,j} - T_{se,j}\right)}{\sum_{j=1}^{n} q_j}, \tag{3}$$

where R_{AM} represents the R-value evaluated by the average method (m^2·K/W), and T_{si} and T_{se} are the interior and exterior surface temperatures (K), respectively.

According to the ISO 9869-1 standard [4], when the estimate is computed after each measurement, an asymptotical value is obtained. If the following three convergence conditions are met simultaneously, this value can be considered to be the actual value, and the test should be terminated. The first convergence condition is that the test duration should exceed 72 h. The second convergence condition is that the R-value obtained at the end of the test does not deviate by more than ±5% from the value obtained 24 h prior to end of the test, as given in Equation (4). The third convergence condition is that the R-value obtained by analyzing data from the first time period during $\mathrm{INT}(2 \times D_T/3)$ days does not deviate by more than ±5% from the values obtained by analyzing data from the last time period of the same duration, as given in Equation (5).

$$\left| \frac{R_{D_T} - R_{D_T - 24h}}{R_{D_T - 24h}} \right| \leq 5\%, \tag{4}$$

$$\left| \frac{R_{INT(2 \times D_T/3),\ first} - R_{INT(2 \times D_T/3),\ last}}{R_{INT(2 \times D_T/3),\ last}} \right| \leq 5\%, \tag{5}$$

where D_T is the duration of the test (days), and INT is the integer part.

In this study, the uncertainty associated with the U-value evaluation was estimated by the combined standard uncertainty determined according to the Guide to the Expression of Uncertainty in Measurement [32] while considering the accuracy of the measurement equipment as well as the operating conditions. The combined standard uncertainty for all the input quantities, which are independent, was obtained as

$$u_c(y) = \sqrt{\sum_{i=1}^{N} \left(\frac{\delta f}{\delta x_i} \right)^2 u^2(x_i)}, \tag{6}$$

where $u_c(y)$ is the combined standard uncertainty, N is the number of input quantities X_i on which the measurand Y depends, f is the functional relationship between the measurand Y and input quantities X_i and between the output estimate y and input estimates x_i on which y depends, $u(x_i)$ is the standard uncertainty of the input estimate x_i, and $\delta f/\delta x_i$ is the sensitivity coefficient (c_i) or partial derivative with respect to the input quantity X_i of the functional relationship f.

As indicated by Equations (2) and (3), the *R*-value and *U*-value are associated with three variables; thus, each value has three sensitivity coefficients. Therefore, the combined standard uncertainties of the *R*-value and *U*-value were obtained by using the corresponding sensitivity coefficients—that is, the partial derivatives, as follows:

$$u_c(R) = \sqrt{\left(\frac{\delta R}{\delta q}\right)^2 u^2(q) + \left(\frac{\delta R}{\delta T_{si}}\right)^2 u^2(T_{si}) + \left(\frac{\delta R}{\delta T_{se}}\right)^2 u^2(T_{se})}, \quad (7)$$

$$u_c(U) = \sqrt{\left(\frac{\delta U}{\delta q}\right)^2 u^2(q) + \left(\frac{\delta U}{\delta T_i}\right)^2 u^2(T_i) + \left(\frac{\delta U}{\delta T_e}\right)^2 u^2(T_e)}. \quad (8)$$

Table 3 lists the uncertainty sources and their contributions toward calculating the standard uncertainty of input quantities. In this study, the uncertainty was expressed using the expanded uncertainty *U*, which was obtained by multiplying the combined standard uncertainty $u_c(y)$ by a coverage factor *k*. The value of the coverage factor was selected as 2, corresponding to a confidence level of 95.45%.

Table 3. Uncertainty sources and their contributions.

Type	Uncertainty Source	Systematic Uncertainty	Random Uncertainty
Instrument	Accuracy of thermocouples	±0.5 °C [1]	
	Accuracy of heat flux sensor	2% [1]	
	Accuracy of data logger	10% [2]	
	Thermocouple calibration	±2.2 °C [1]	
	Heat flux sensor calibration	3% [1]	
Operation	Poor contact between thermocouple and surface		5% [2]
	Poor contact between heat flux sensor and surface		5% [2]
	Modification of isotherms caused by heat flux sensor		2%–3% [2]
	Variation in temperatures and heat flux over time		±10% [2]

[1] Uncertainty value according to manufacturer's technical specifications. [2] Uncertainty value according to ISO 9869-1 [4].

3. Results and Discussion

3.1. Evolution of R-Value and U-Value

Figure 3 shows the evolution of the in situ *R*-value and *U*-value over the total test duration of 21 consecutive days with their corresponding expanded uncertainties analyzed in a cycle of 1 day using the average method. The in situ *R*-value and *U*-value tended to stabilize around the final values from the 12th day of the test. The *R*-value and *U*-value obtained at the end of the test were 0.988 ± 0.009 m^2·K/W and 0.908 ± 0.007 W/m^2·K, respectively, which are, respectively, 51.1% smaller and 113.0% larger than the theoretical values calculated according to the ISO 6946 standard. These results show that the thermal performance of the test wall deteriorated considerably for approximately 28 years after completion, and that it was necessary to measure the thermal performance of the wall onsite.

For the asymptotic values to be considered as the *R*-value and *U*-value, the three conditions mentioned in Section 2.3 must be satisfied. Tables 4 and 5 summarize the values used for determining the convergence of the *R*-value and *U*-value calculated by the average method, respectively. The deviation of the *R*-value and *U*-value according to the second and third convergence conditions is shown in Figure 4.

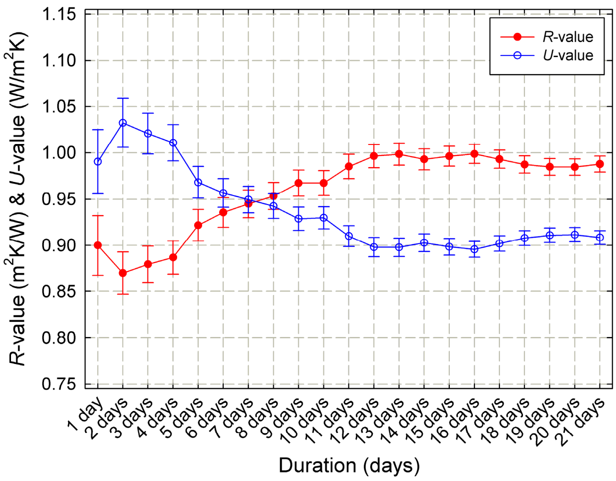

Figure 3. Evolution of in situ *R*-value and *U*-value with their expanded uncertainties.

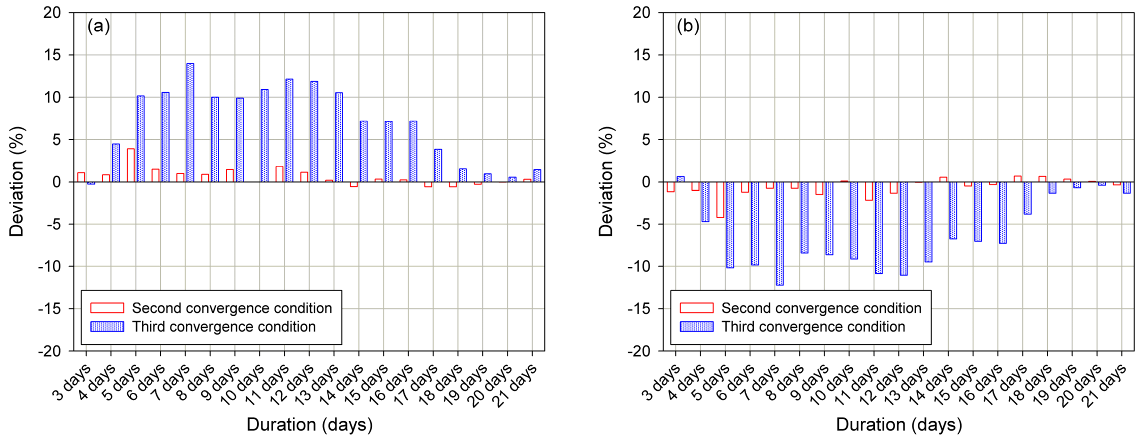

Figure 4. Deviation of (**a**) *R*-value and (**b**) *U*-value according to convergence conditions of the ISO 9869-1 standard.

As can be seen in Figure 4, the second condition that the deviation between the value obtained at the end of the test, and the value obtained 24 h before should be within ±5%, which is easily satisfied because there is no major difference in the data used for the calculation of the cumulative average. However, deviations for the third convergence condition according to Equation (5) are considerably larger than deviations for the second convergence condition. The decrease in the deviation with an increase in the analysis period is also not clear, and the third convergence condition was satisfied only 17 days after the start of measurement. These results were obtained because the analysis period was shortened from D_T to $\mathrm{INT}(2 \times D_T/3)$, and the deviations of the *R*-value and *U*-value were calculated between the initial and latter periods of the same duration. The overlap period for the second convergence condition continued to increase proportionally as the measurement period became longer, but the overlap period for the third convergence condition did not exceed 50% of the comparison period. Therefore, to easily satisfy the third convergence condition, there should be slight changes in the environmental variables in the two periods.

As can be seen in Figure 2a, the temperature difference across the test wall during the entire test period tended to decrease at the beginning, then remained constant, and finally increased again. Though the test was conducted under a large temperature difference and stable environment as recommended in previous studies [7,12–14,33] and the ISO 9869-1 standard [4], the difficulty in satisfying the third convergence condition is attributed to these changes in the temperature differences during the entire test period. The results show that the third convergence condition is satisfied by the influence of cumulative averaging over a sufficiently long analysis period accompanied by an increase in the measurement period. For example, for the third convergence condition, the analysis period corresponding to the measurement period of 17 days in which the variation was stable within ±5% was 11 days, which is considerably longer than the test duration of previous studies [7,8,12,14,28].

When the measurement period is three and four days, both the convergence conditions are satisfied, but the deviations of the *R*-value and *U*-value obtained at the end of the test are more than 10%. The *R*-value and *U*-value whose deviations are within ±5% of their corresponding final values are derived from data obtained after the 7th day; however, both convergence conditions were satisfied only from the 17th day. Therefore, it is considered that the criteria for determining convergence by the average method based on ISO 9869-1 [4], particularly the third convergence condition, are very strict.

As can be observed in Tables 4 and 5, the duration of the test affects the measurement uncertainties. For *U*-values analyzed with their expanded uncertainties in Table 5, the measurement uncertainties decreased from ±0.022 W/m^2·K on the third day to ±0.007 W/m^2·K at the end of the test when the duration of the test was extended. This tendency is commonly confirmed in the *R*-values in Table 4. These results are in good agreement with the results in previous studies in [7,12,16,28], showing that an increase in the measurement period improves the measurement accuracy.

Table 4. *R*-values analyzed by average method and their expanded uncertainties.

D_T (days)	$INT(2 \times D_T/3)$ (days)	R-values with Their Expended Uncertainties (m^2·K/W)			
		R_{D_T}	R_{D_T-24h}	$R_{INT(2\times D_T/3), first}$	$R_{INT(2\times D_T/3), last}$
3	2	0.879 ± 0.020	0.870 ± 0.023	0.870 ± 0.023	0.868 ± 0.025
4	2	0.887 ± 0.018	0.879 ± 0.020	0.870 ± 0.023	0.909 ± 0.029
5	3	0.922 ± 0.017	0.887 ± 0.018	0.879 ± 0.020	0.969 ± 0.025
6	4	0.936 ± 0.016	0.922 ± 0.017	0.887 ± 0.018	0.980 ± 0.022
7	4	0.945 ± 0.015	0.936 ± 0.016	0.887 ± 0.018	1.011 ± 0.023
8	5	0.954 ± 0.015	0.945 ± 0.015	0.922 ± 0.017	1.014 ± 0.021
9	6	0.967 ± 0.014	0.954 ± 0.015	0.936 ± 0.016	1.028 ± 0.020
10	6	0.967 ± 0.013	0.967 ± 0.014	0.936 ± 0.016	1.038 ± 0.020
11	7	0.985 ± 0.013	0.967 ± 0.013	0.945 ± 0.015	1.060 ± 0.019
12	8	0.996 ± 0.013	0.985 ± 0.013	0.954 ± 0.015	1.067 ± 0.017
13	8	0.998 ± 0.012	0.996 ± 0.013	0.954 ± 0.015	1.054 ± 0.016
14	9	0.993 ± 0.011	0.998 ± 0.012	0.967 ± 0.014	1.037 ± 0.015
15	10	0.996 ± 0.011	0.993 ± 0.011	0.967 ± 0.013	1.037 ± 0.014
16	10	0.999 ± 0.010	0.996 ± 0.011	0.967 ± 0.013	1.037 ± 0.013
17	11	0.993 ± 0.010	0.999 ± 0.010	0.985 ± 0.013	1.023 ± 0.012
18	12	0.987 ± 0.009	0.993 ± 0.010	0.996 ± 0.013	1.012 ± 0.011
19	12	0.985 ± 0.009	0.987 ± 0.009	0.996 ± 0.013	1.006 ± 0.011
20	13	0.985 ± 0.009	0.985 ± 0.009	0.998 ± 0.012	1.004 ± 0.011
21	14	0.988 ± 0.009	0.985 ± 0.009	0.993 ± 0.011	1.007 ± 0.010

Table 5. *U*-values analyzed by average method and their expanded uncertainties.

D_T (days)	$INT(2 \times D_T/3)$ (days)	*U*-values with Their Expended Uncertainties (W/ m^2·K)			
		U_{D_T}	U_{D_T-24h}	$U_{INT(2\times D_T/3), first}$	$U_{INT(2\times D_T/3), last}$
3	2	1.021 ± 0.022	1.032 ± 0.026	1.032 ± 0.026	1.039 ± 0.029
4	2	1.011 ± 0.020	1.021 ± 0.022	1.032 ± 0.026	0.984 ± 0.030
5	3	0.968 ± 0.017	1.011 ± 0.020	1.021 ± 0.022	0.917 ± 0.022
6	4	0.957 ± 0.015	0.968 ± 0.017	1.011 ± 0.020	0.911 ± 0.019
7	4	0.950 ± 0.014	0.957 ± 0.015	1.011 ± 0.020	0.887 ± 0.019
8	5	0.942 ± 0.013	0.950 ± 0.014	0.968 ± 0.017	0.887 ± 0.017
9	6	0.929 ± 0.013	0.942 ± 0.013	0.957 ± 0.015	0.874 ± 0.015
10	6	0.930 ± 0.012	0.929 ± 0.013	0.957 ± 0.015	0.869 ± 0.015
11	7	0.910 ± 0.011	0.930 ± 0.012	0.950 ± 0.014	0.846 ± 0.014
12	8	0.898 ± 0.010	0.910 ± 0.011	0.942 ± 0.013	0.838 ± 0.012
13	8	0.898 ± 0.010	0.898 ± 0.010	0.942 ± 0.013	0.853 ± 0.012

Table 5. *Cont.*

D_T (days)	$INT(2\times D_T/3)$ (days)	U-values with Their Expended Uncertainties (W/ m^2·K)			
		U_{D_T}	U_{D_T-24h}	$U_{INT(2\times D_T/3),\,first}$	$U_{INT(2\times D_T/3),\,last}$
14	9	0.903 ± 0.010	0.898 ± 0.010	0.929 ± 0.013	0.866 ± 0.011
15	10	0.898 ± 0.009	0.903 ± 0.010	0.930 ± 0.012	0.865 ± 0.011
16	10	0.896 ± 0.009	0.898 ± 0.009	0.930 ± 0.012	0.862 ± 0.010
17	11	0.902 ± 0.008	0.896 ± 0.009	0.910 ± 0.011	0.875 ± 0.010
18	12	0.908 ± 0.008	0.902 ± 0.008	0.898 ± 0.010	0.886 ± 0.009
19	12	0.911 ± 0.008	0.908 ± 0.008	0.898 ± 0.010	0.892 ± 0.009
20	13	0.912 ± 0.008	0.911 ± 0.008	0.898 ± 0.010	0.894 ± 0.009
21	14	0.908 ± 0.007	0.912 ± 0.008	0.903 ± 0.010	0.891 ± 0.009

3.2. *Effect of Variation in Analysis Period*

Reliable results can be obtained when the measurement is conducted using the heat flow meter method under stable environmental conditions such as a high temperature difference across the test wall, low wind speed, and an avoidance of direct solar radiation. However, the period in which the above stable environmental conditions are satisfied is actually not long. In addition, measurements conducted in buildings where residents are living cause inconvenience to their daily lives. Therefore, it is difficult to measure the in situ R-value and U-value of a wall for a long period of time for many buildings.

In this study, for a single measurement campaign of 21 days, we reviewed the convergence characteristics of the in situ R-value and U-value under the assumption that many measurements are conducted on the same test wall by shifting the measurement start date by 1 day and setting the analysis period to be different. For example, if the analysis period is set to 3 days and the period is continuously moved forward by 1 day from the start date of the test, 19 tests can be considered to have been conducted. In this example, out of the 19 cases, there are seven cases (37%) where no days are duplicated and 10 cases (53%) where 1 day is duplicated. As all days during the original measurement period of 21 days met the recommended environmental conditions, the approach proposed in this study can be considered reasonable. Therefore, this approach can be used to study the convergence characteristics of the in situ R-value and U-value according to variation in the analysis period under the aforementioned constraints. However, this approach has limitations in that the number of cases decreases as the analysis period becomes longer and the environmental variables in these cases become similar to each other because of overlap.

Figure 5 shows the R-values and U-values evaluated according to the approach described above for different analysis periods. The shorter the analysis period, the larger the dispersion of the R-values and U-values. As the analysis period becomes longer, these values tended to converge near the final values analyzed using the measurement data for 21 days. In addition, the percentages of cases deviating by more than ±5% from the final values were as high as approximately 40% when the analysis period was short; however, these percentages gradually decreased, and such cases were not found when the analysis period was longer than 13 days.

The convergence of the R-values and U-values obtained for different analysis periods was examined according to the two convergence conditions of the ISO 9869-1 standard, and the results are shown in Figures 6 and 7. The second convergence condition, which compares the deviation of the two values with a 24 h difference, is unsatisfactory only in three cases for the R-values and four cases for the U-values among the cases with analysis periods of 3 and 4 days. This is because when the measurement is conducted in a stable environment, as is the case in this study, a rapid change exceeding more than ±5% is unlikely to occur, considering a 24 h difference. On the other hand, the third convergence condition is not met in any of the cases until the analysis period is 16 days, and the deviation is also very large compared to that in the second condition. These results indicate that the fulfillment of the convergence conditions according to the ISO 9869-1 standard is largely dependent on the third condition. In other words, to obtain reliable results in a short period of time, it is necessary to keep the environmental variables constant throughout the measurement period, or an appropriate period must be selected.

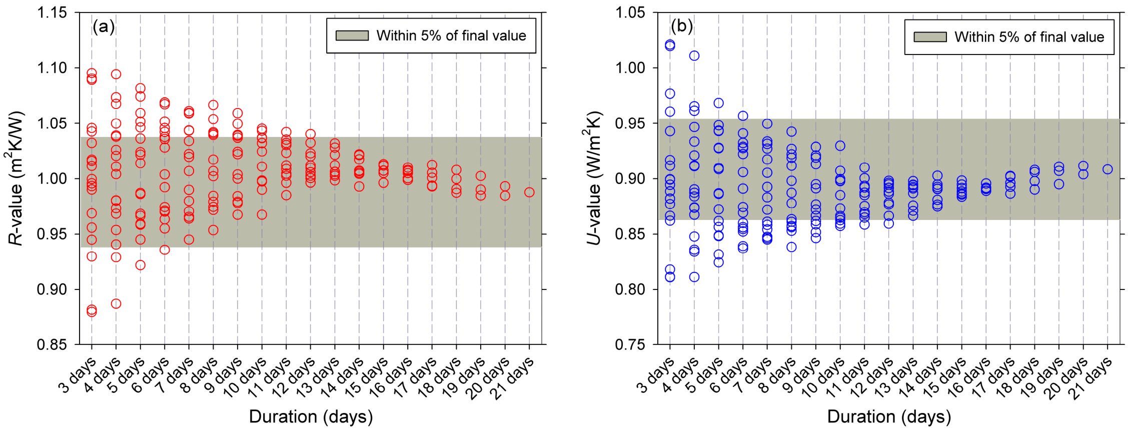

Figure 5. Distributions of (**a**) *R*-values and (**b**) *U*-values evaluated for different analysis periods.

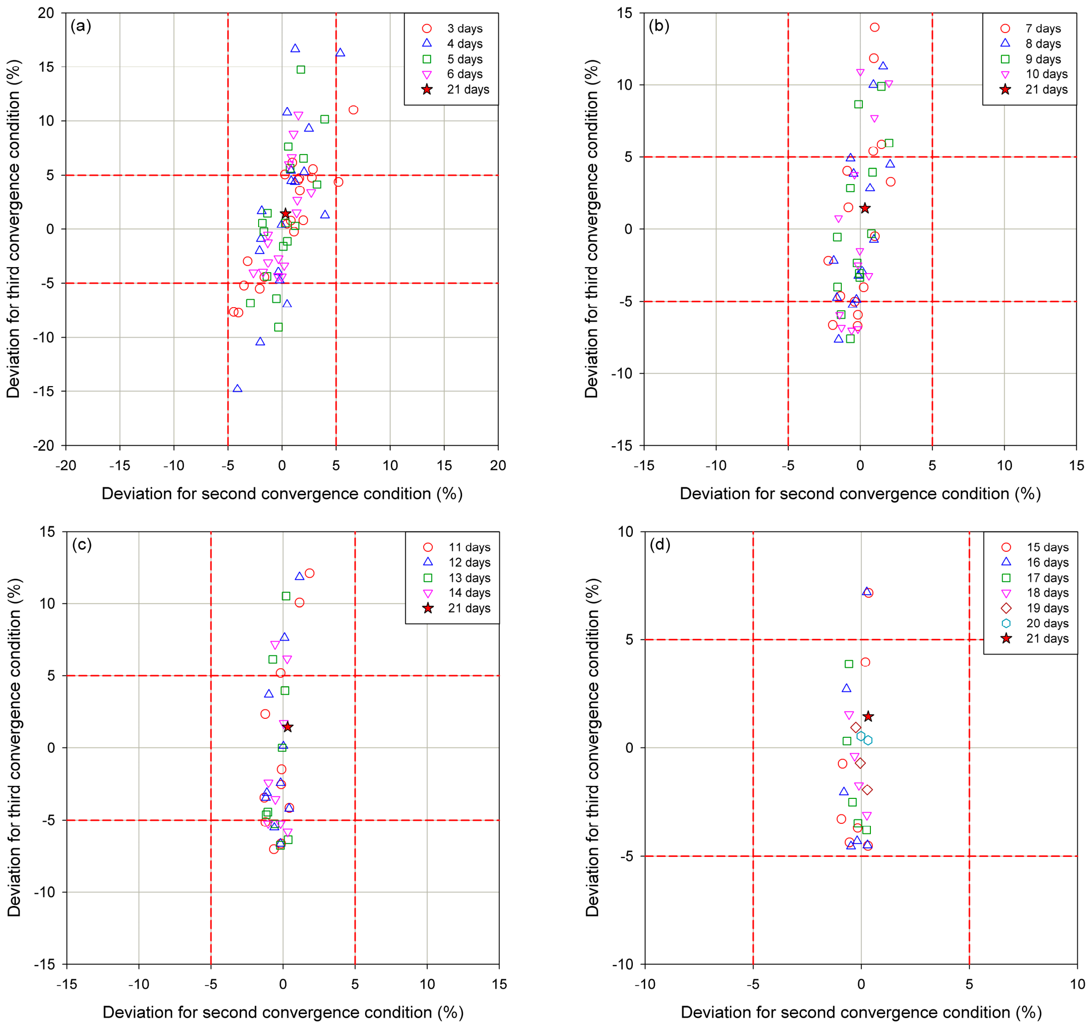

Figure 6. Convergence characteristics of *R*-values evaluated for different analysis periods according to conditions of the ISO 9869-1 standard. For ease of understanding, the plots are divided into four sub-figures based on the length of the analysis period: (**a**) 3–6 days; (**b**) 7–10 days; (**c**) 11–14 days; (**d**) 15–20 days.

As shown in Figure 5, the *R*-values and *U*-values in all the cases with an analysis period of 13 days or more were within ±5% of the respective final values. However, Figures 6 and 7 show that both convergence conditions begin to be satisfied in the cases where the analysis period is more than 17 days. Therefore, the findings show that a minimum test duration of more than 2 weeks is required, even if the daily air temperature difference is maintained at a minimum of 16.5 °C throughout the entire test duration and the environmental variables are not changed considerably.

According to the average method based on the ISO 9869-1 standard [4], the test may be ended only when the convergence conditions obtained using the *R*-value are fulfilled. In this study, two convergence conditions were analyzed using both the *R*-value and *U*-value, and very similar convergence characteristics were identified. As can be observed in Figures 6 and 7, the deviations for the two convergence conditions appear symmetrical because the *R*-value and *U*-value are essentially reciprocal. However, except for the deviations with symmetrical form, other aspects such as the fulfillment of the convergence conditions and the proportion of cases for which the convergence conditions are fulfilled were very similar for the two values. Therefore, the findings show that it is possible to determine the end of the test, that is its convergence, using the U-value instead of the R-value.

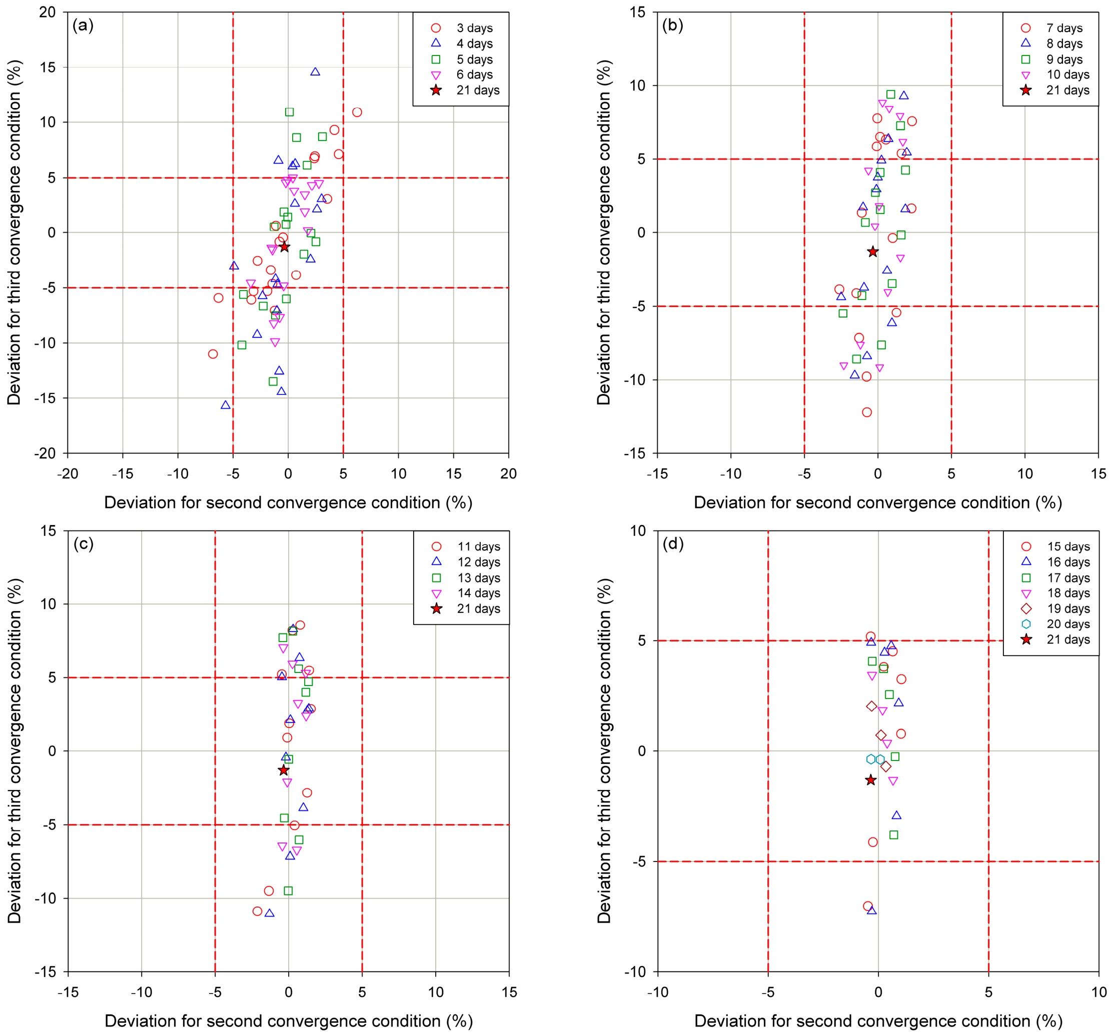

Figure 7. Convergence characteristics of *U*-values evaluated for different analysis periods according to conditions of the ISO 9869-1 standard. For ease of understanding, the plots are divided into four sub-figures based on the length of the analysis period: (**a**) 3–6 days; (**b**) 7–10 days; (**c**) 11–14 days; (**d**) 15–20 days.

3.3. Effect of Temperature Difference

A large temperature difference between the inside and outside environments has often been referred to as one of the key factors to obtain reliable results through the heat flow meter method. Thus, the influence of the temperature difference on the accuracy of the results derived from different analysis periods was analyzed. Figure 8 shows the average surface and air temperature differences between the inside and outside environments for different analysis periods described in Section 3.2. As the analysis period decreased, the average temperature differences showed dispersed distribution because of changes in the outside air temperature throughout the test duration. When the analysis period was 3 days, the surface temperature differences were in the range of approximately 15.5–24.8 °C, and the air temperature differences were in the range of approximately 17.1–27.7 °C. These temperature differences gradually became similar and reached the average temperature differences of the entire test period, namely 19.6 °C and 21.8 °C, because of the influence of the cumulative average as the analysis periods increased. These temperature differences across the test wall were considerably higher than the temperature condition—that is, 10.0 °C—recommended by the ISO 9869-1 standard [4].

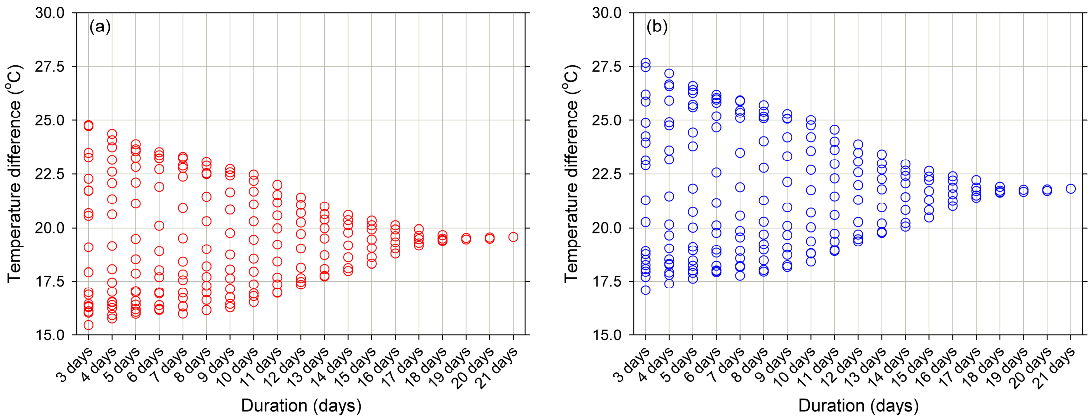

Figure 8. Average (**a**) surface and (**b**) air temperature differences between inside and outside environments for different analysis periods.

The average temperature differences and the corresponding *R*-values and *U*-values for different analysis periods are plotted in Figures 9 and 10, respectively. In the cases where the average surface temperature difference was more than 19.6 °C, the *R*-values were mostly within ±5% of the value derived at the end of the test. On the other hand, in the cases where the average surface temperature difference was less than 19.6 °C, the *R*-values that deviate by more than ±5% from the final value were more frequently found than in the other cases. For example, for an analysis period of 3 days, there were nine cases where the average surface temperature difference was greater than 19.6 °C, and only two of these cases showed deviations greater than ±5% from the final value. In contrast, six out of the 10 cases with an average surface temperature difference below 19.6 °C had deviations outside the ±5% range. As can be observed in Figure 9a,b, this tendency is commonly confirmed in cases where the analysis period is relatively short. Therefore, the results show that if the test duration is the same, the larger the surface temperature difference and the greater the possibility of causing a lower deviation.

The *R*-values for all the cases with an analysis period of 13 days or more converged within ±5% of the final value without a large influence of the surface temperature difference between the inside and outside environments. Therefore, if the surface temperature difference is higher than a certain temperature difference—that is, 10 °C—recommended in previous studies [7,33] and the ISO 9869-1 standard [4], the convergence of the *R*-values is affected more by the length of the analysis period than by the surface temperature difference. These results are also seen in the relationship between the *U*-values and the air temperature differences between the inside and outside environments (Figure 10). However, these analysis results still have limitations in that measurement data for 21 days were used; thus, further research based on long-term measurements is needed.

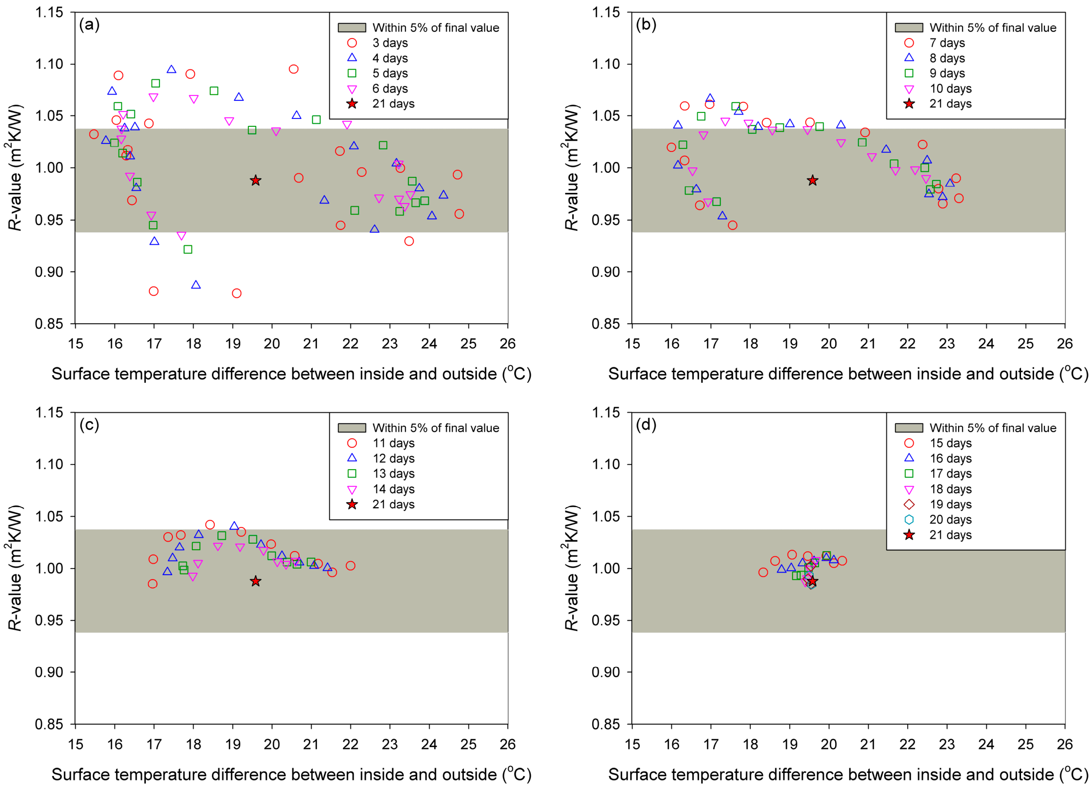

Figure 9. Relationship between average surface temperature differences and final *R*-values evaluated for different analysis periods. For ease of understanding, the plots are divided into four sub-figures based on the length of the analysis period: (**a**) 3–6 days; (**b**) 7–10 days; (**c**) 11–14 days; (**d**) 15–20 days.

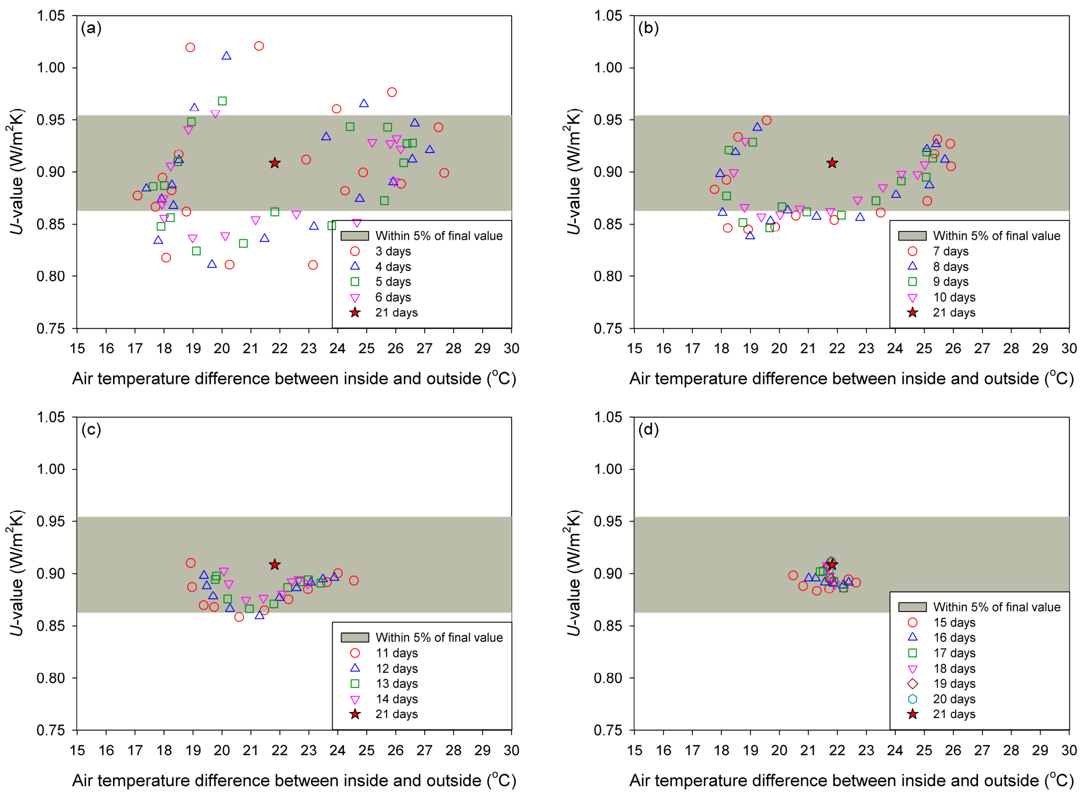

Figure 10. Relationship between average air temperature differences and final *U*-values evaluated for different analysis periods. For ease of understanding, the plots are divided into four sub-figures based on the length of the analysis period: (**a**) 3–6 days; (**b**) 7–10 days; (**c**) 11–14 days; (**d**) 15–20 days.

4. Conclusions

This study evaluated the convergence characteristics of the in situ *R*-value and *U*-value analyzed using the standardized average method. The convergence characteristics were analyzed according to the convergence criteria regulated by ISO 9869-1 [4]. Onsite measurement was conducted on the northwest-facing external wall for over 21 days in winter under fairly stable environmental conditions, as recommended by ISO 9869-1 [4] and the literature [7,12–14,33]. To analyze the effect of the length of the analysis period and the temperature difference on the convergence characteristics of the in situ *R*-value and *U*-value, datasets for different analysis periods were created from the onsite measurement data for 21 consecutive days.

Our results show that in situ *R*-values and *U*-values that were within ±5% of the values obtained across a full test duration were obtained starting from the 7th day, but the convergence conditions were satisfied only from the 17th day. This is because the length of the overlap period and the periods used for comparing the deviations are different between the second and third convergence conditions. The overlap period for the second condition increases proportionally as the measurement period becomes longer, but, in the third condition, the overlap period does not exceed 50% of the comparison period. This result indicates that the convergence according to the ISO 9869-1 standard largely depends on the third condition. Therefore, to obtain reliable in situ *R*-values and *U*-values in a short test duration, it is necessary to keep the environmental variables constant throughout the entire test duration, or an appropriate duration should be selected.

Our results also show that when the test duration is relatively short, the larger the temperature difference and the smaller the deviation for the convergence conditions. However, when the test duration is longer (approximately 2 weeks or more in this study), the effect of the temperature difference on the convergence of the in situ *R*-value and *U*-value decreases gradually because of cumulative averaging. Therefore, if the temperature difference is higher than the recommended value—that is, 10 °C—the convergence of the in situ *R*-value and *U*-value is affected more by the length of the test duration than by the temperature difference.

In addition, our findings indicate that for the in situ *R*-value and *U*-value, although the deviation values for the convergence conditions are symmetrical, other aspects such as the fulfillment of the convergence conditions and the proportion of cases for which the convergence conditions are fulfilled are very similar for the two values. Therefore, it is found that there is no difference between the use of the *R*-value and *U*-value in determining the end of the test.

In this study, it is assumed that many measurements were conducted on the same test wall by creating datasets for different analysis periods from a single onsite measurement dataset for 21 consecutive days. Thus, we intend to conduct further research by increasing the number of test walls and using onsite measurement data for longer periods. Furthermore, we intend to investigate the selection of an appropriate test duration and how the duration should be shortened.

Author Contributions: Conceptualization, D.S.C. and M.J.K.; methodology, M.J.K.; validation, D.S.C.; formal analysis, D.S.C. and M.J.K.; investigation, M.J.K.; data curation, M.J.K.; writing—original draft preparation, M.J.K.; writing—review and editing, D.S.C. and M.J.K.; visualization, M.J.K.; supervision, D.S.C.; project administration, D.S.C.; funding acquisition, D.S.C.

Funding: This research was supported by an Academic Research Fund of Chungwoon University in 2017 and Basic Science Research Program through the National Research Foundation of Korea (NRF) funded by the Ministry of Education (NRF-2017R1D1A1B03034281).

Conflicts of Interest: The authors declare no conflict of interest.

Nomenclature

D_T	Test duration, days
f	Functional relationship between measurand Y and input quantities X_i on which measurand Y depends
INT	Integer part
j	Individual measurements
n	Number of measurement data points
N	Number of input quantities X_i on which measurand Y depends
q_j	Density of heat flow rate, W/m^2
R_{AM}	Thermal resistance value evaluated by average method, m^2·K/W
R_{si}	Interior surface resistance, m^2·K/W
R_{se}	Exterior surface resistance, m^2·K/W
t.	Material thickness, m
$T_{e,j}$	Exterior air temrature, K
$T_{i,j}$	Interior air temperature, K
$T_{se,j}$	Exterior wall surface temperature, K
$T_{si,j}$	Interior wall surface temperature, K
$u_c(y)$	Combined standard uncertainty
$u(x_i)$	Standard uncertainty of input estimate x_i
U_{AM}	Thermal transmittance value evaluated by average method, W/m^2·K
U_D	Thermal transmittance value evaluated by calculation method, W/m^2·K
X_i	ith input quantity on which measurand Y depends
x_i	Estimate of input X_i
Y	Measurand
y	Estimate of measurand Y
λ	Thermal conductivity, W/m·K

References

1. Ministry of Land, Infrastructure and Transport (MOLIT). *Energy Saving Design Standards for Building*; Ministry of Land, Infrastructure and Transport: Sejong, Korea, 2017. Available online: http://www.molit.go.kr/USR/I0204/m_45/dtl.jsp?idx=15270 (accessed on 19 February 2019).
2. ISO 6946:2007—Building Components and Building Elements—Thermal Resistance and Thermal Transmittance—Calculation Method. Available online: https://www.iso.org/standard/65708.html (accessed on 19 February 2019).
3. Choi, D.S.; Ko, M.J. Comparison of various analysis methods based on heat flowmeters and infrared thermography measurements for the evaluation of the in situ thermal transmittance of opaque exterior walls. *Energies* **2017**, *10*, 1019. [CrossRef]
4. ISO 9869–1:2014. Building Elements—In-Situ Measurement of Thermal Resistance and Thermal Transmittance—Part 1: Heat Flow Meter Method. Available online: https://www.iso.org/standard/59697.html (accessed on 19 February 2019).
5. Adhikari, R.S.; Lucchi, E.; Pracchi, V. Experimental measurements on thermal transmittance of the opaque vertical walls in the historical buildings. In Proceedings of the 28th International PLEA Conference on Sustainable Architecture + Urban Design, Lima, Peru, 7–9 November 2012.
6. Cabeza, L.F.; Castell, A.; Medrano, M.; Martorell, I.; Perez, G.; Fernandez, I. Experimental study on the performance of insulation materials in mediterranean construction. *Energy Build.* **2010**, *42*, 630–636. [CrossRef]
7. Asdrubali, F.; D'Alessandro, F.; Baldinelli, G.; Bianchi, F. Evaluating in situ thermal transmittance of green buildings masonries—A case study. *Case Stud. Constr. Mater.* **2014**, *1*, 53–59. [CrossRef]
8. Evangelisti, L.; Guattari, C.; Gori, P.; Vollaro, R.D.L. In situ thermal transmittance measurements for investigating differences between wall models and actual building performance. *Sustainability* **2015**, *7*, 10388–10398. [CrossRef]

9. Baker, P. *U-Value and Traditional Buildings: In Situ Measurements and Their Comparisons to Calculated Values*; Historic Scotland Technical Paper: Edinburgh, UK, 2011.
10. Rye, C.; Scott, C. The SPAB Research Report 1: U-Value Report. Society for the Protection of Ancient Buildings, London. 2012. Available online: https://www.spab.org.uk/sites/default/files/documents/MainSociety/Advice/SPABU-valueReport.Nov2012.v2.pdf (accessed on 19 February 2019).
11. Bros-Williamson, J.; Carnier, C.; Currie, J.I. A longitudinal building fabric and energy performance analysis of two homes built to different energy principles. *Energy Build.* **2016**, *130*, 578–591. [CrossRef]
12. Gaspar, K.; Casals, M.; Gangolells, M. In situ measurement of façades with a low U-value: Avoiding deviations. *Energy Build.* **2018**, *170*, 61–73. [CrossRef]
13. Ahmad, A.; Maslehuddin, M.; Al-Hadhrami, L.M. In situ measurement of thermal transmittance and thermal resistance of hollow reinforced precast concrete walls. *Energy Build.* **2014**, *84*, 132–141. [CrossRef]
14. Ficco, G.; Iannetta, F.; Ianniello, E.; d'Ambrosio Alfano, F.R.; Dell'Isola, M. U-value in situ measurement for energy diagnosis of existing buildings. *Energy Build.* **2015**, *104*, 108–121. [CrossRef]
15. Deconinck, A.H.; Roels, S. Comparison of characterization methods determining the thermal resistance of building components from onsite measurements. *Energy Build.* **2016**, *130*, 309–320. [CrossRef]
16. Gaspar, K.; Casals, M.; Gangolells, M. Review of criteria for determining HFM minimum test duration. *Energy Build.* **2018**, *176*, 360–370. [CrossRef]
17. ASTM C 1155. Standard Practice for Determining Thermal Resistance of Building Envelope Components from the In-Situ Data. Available online: https://www.astm.org/Standards/C1155.htm (accessed on 19 February 2019).
18. Haralambopoulos, D.A.; Paparsenos, G.F. Assessing the thermal insulation of old buildings—The need for in situ spot measurements of thermal resistance and planar infrared thermography. *Energy Convers. Manag.* **1998**, *39*, 65–79. [CrossRef]
19. Balaras, C.A.; Argiriou, A.A. Infrared thermography for building diagnostics. *Energy Build.* **2002**, *34*, 171–183. [CrossRef]
20. Ocana, S.M.; Guerrero, I.C.; Requena, I.G. Thermographic survey of two rural buildings in Spain. *Energy Build.* **2004**, *36*, 515–523. [CrossRef]
21. Kalamees, T. Air tightness and air leakages of new lightweight single-family detached houses in Estonia. *Build. Environ.* **2007**, *42*, 2369–2377. [CrossRef]
22. Taylor, T.; Counsell, J.; Gill, S. Energy efficiency is more than skin deep: Improving construction quality control in new-build housing using thermography. *Energy Build.* **2013**, *66*, 222–231. [CrossRef]
23. Albatici, R.; Tonelli, A.M. Infrared thermovision technique for the assessment of the thermal transmittance value of opaque building elements on site. *Energy Build.* **2010**, *42*, 2177–2183. [CrossRef]
24. Albatici, R.; Tonelli, A.M.; Chiogna, M. A comprehensive experimental approach for the validation of quantitative infrared thermography in the evaluation of building thermal transmittance. *Appl. Energy* **2015**, *141*, 218–228. [CrossRef]
25. Fokaides, P.A.; Kalogirou, S.A. Application of infrared thermography for the determination of the overall heat transfer coefficient (U-value) in building envelopes. *Appl. Energy* **2011**, *88*, 4358–4365. [CrossRef]
26. Dall'O, G.; Sarto, L.; Panza, A. Infrared screening of residential buildings for energy audit purposes: Results of a field test. *Energies* **2013**, *6*, 3859–3878. [CrossRef]
27. Nardi, I.; Sfarra, S.; Ambrosini, D. Quantitative thermography for the estimation of the U-value: State of the art and a case study. In Proceedings of the 32nd UIT (Italian Union of Thermo-fluid-dynamics) Heat Transfer Conference, Pisa, Italy, 23–25 June 2014. [CrossRef]
28. Nardi, I.; Ambrosini, D.; Rubeis, T.D.; Sfarra, S.; Perilli, S.; Pasqualoni, G. A comparison between thermographic and flow-meter methods for the evaluation of thermal transmittance of different wall constructions. In Proceedings of the 33th UIT (Italian Union of Thermo-fluid-dynamics) Heat Transfer Conference, L'Aquila, Italy, 22–24 June 2015. [CrossRef]
29. Biddulph, P.; Gori, V.; Elwell, C.; Scott, C.; Rye, C.; Lowe, R.; Oreszczyn, T. Inferring the thermal resistance and effective thermal mass of a wall using frequent temperature and heat flux measurements. *Energy Build.* **2014**, *78*, 10–16. [CrossRef]
30. Gori, V.; Marincioni, V.; Biddulph, P.; Elwell, C.A. Inferring the thermal resistance and effective thermal mass distribution of a wall from in situ measurements to characterize heat transfer at both the interior and exterior surfaces. *Energy Build.* **2017**, *135*, 398–409. [CrossRef]

31. Iglesias, M.; Sawlan, Z.; Scavino, M.; Tempone, R.; Wood, C. Bayesian inferences of the thermal properties of a wall using temperature and heat flux measurements. *Int. J. Heat Mass Transf.* **2018**, *116*, 417–431. [CrossRef]
32. ISO/IEC Guide 98–9:2008. Uncertainty of Measurement—Part 3: Guide to the Expression of Uncertainty in Measurement. Available online: https://www.iso.org/standard/50461.html (accessed on 19 February 2019).
33. Desogus, G.; Mura, S.; Ricciu, R. Comparing different approaches to in situ measurement of building components thermal resistance. *Energy Build.* **2011**, *43*, 2613–2620. [CrossRef]

© 2019 by the authors. Licensee MDPI, Basel, Switzerland. This article is an open access article distributed under the terms and conditions of the Creative Commons Attribution (CC BY) license (http://creativecommons.org/licenses/by/4.0/).